*Journal of Thermal Analysis Vol. 46 (1996) 719-731*

Dedicated to Professor Bernhard Wunderlich on the occasion of his 65th birthday

# THE CRYSTAL STRUCTURES AND THERMAL SHRINKAGE PROPERTIES OF AROMATIC POLYIMIDE FIBERS

*Z. Wu, A. Zhang, D. Shen, M. Leland, F. W. Harris and S. Z. D. Cheng*

Maurice Morton Institute and Department of Polymer Science, The University of Akron, Akron, Ohio, 44325-3909, USA

## Abstract

Three aromatic polyimides based on 3,3',4,4'-biphenyl-tetracarboxylic dianhydride (BPDA) and three different diamines 2,2'-bis(trifluoromethyl)-4,4'-diaminobiphenyl (PFMB), 2,2'-dimethyl-4,4'-diaminophenyl (DMB) or 3,3'-dimethylbenzidine (OTOL) have been synthesized. These polyimides are soluble in hot *p*-chlorophenol, *m*-cresol or other phenolic solvents. Fibers have been spun from isotropic solutions using a dry-jet wet spinning method. The as-spun fibers generally exhibit low tensile properties, and can be drawn at elevated temperatures ( >380°C) up to a draw ratio of 10 times. Remarkable increases in tensile strength and modulus are achieved after drawing and annealing. The crystal structures of highly drawn fibers were determined *via* wide angle X-ray diffraction (WAXD). The crystal unit cell lattices have been determined to be monoclinic for BPDA-PFMB and triclinic for both BPDA-DMB and BPDA-OTOL. Thermomechanical analysis (TMA) was used to measure thermal shrinkage stress and strain. A self-elongation has been found in the temperature region around 450°C. This phenomenon can be explained as resulting from the structural development in the fibers as evidenced *via* WAXD observations.

**Keywords:** aromatic polyimide fiber, as-spun fiber, crystallization, crystal structure, crystal unit cell, draw ratio, dry-jet wet spinning, isotropic solution, modulus, self-elongation, tensile strength, thermal shrinkage stress, thermal shrinkage strain, thermomechnical analysis, triclinic, wide angle X-ray diffraction, zone drawing

## Introduction

In previous publications, a series of high performance (high temperature, high modulus, high strength) polyimide fibers has been reported and discussed [1–4]. The first paper of this series reported a new high-performance aromatic polyimide fiber synthesized from 3,3',4,4'-biphenyltetracarboxylic dianhydride (BPDA) and 2,2'-bis(tri-fluoromethyl)-4,4'-diaminobiphenyl (PFMB) in *m*-cresol at elevated temperatures [1]. The chemical structure of BPDA-PFMB is

*0368–4466/96/ $ 5.00*

*John Wiley & Sons, Limited*
*Chichester*

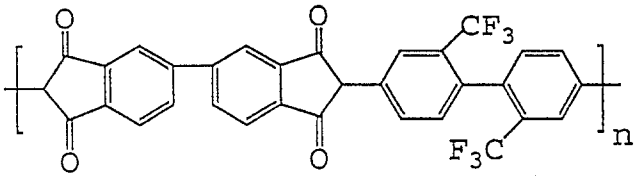

The BPDA-PFMB fibers were spun *via* a dry-jet wet spinning method. The as-spun fibers possess low tenacity and modulus. Extensive drawing can be carried out at elevated temperatures to increase structural orientation and crystallinity. Highly drawn BPDA-PFMB fibers display distinct wide angle X-ray diffraction (WAXD) patterns and a monoclinic unit cell has been determined [1]. The changes in structural parameters such as crystallinity, orientation, and apparent crystallite size under different draw ratios have been studied. With increasing the draw ratio, the mechanical properties of BPDA-PFMB fibers are significantly improved. The fibers with a draw ratio of seven to ten show a tensile strength of 3.2 GPa and a modulus of 130 GPa. BPDA-PFMB fibers also exhibit excellent thermal stability and retain relatively high tensile strengths and moduli at elevated temperatures [1, 2].

After the development of the BPDA-PFMB fiber, a new high molecular weight aromatic polyimide was synthesized from 3,3″,4,4′-biphenyltetracarboxylic dianhydride (BPDA) and 2,2′-dimethyl-4,4′-diaminobiphenyl (DMB) in *p*-chlorophenol at elevated temperatures. This polymer is relatively economical compared with BPDA-PFMB fibers and it is an excellent candidate for use as a high performance polyimide fibers [3]. The chemical structure is

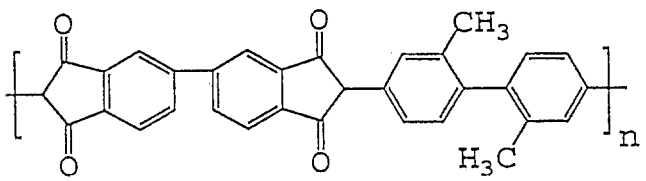

The as-spun fibers also possess low tenacity and modulus. After drawing at 400°C however, BPDA-DMB fibers exhibit tensile properties slightly better than those of BPDA-PFMB fibers. The WAXD pattern of BPDA-DMB fibers indicates a triclinic unit cell [3].

The third aromatic polyimide was synthesized from 3,3′,4,4′-biphenyl-tetracarboxylic dianhydride (BPDA) and 3,3′-dimethylbenzidine (OTOL) in *p*-chlorophenyl. The dry-jet wet spinning method was again used followed by drawing at elevated temperatures. The chemical structure is

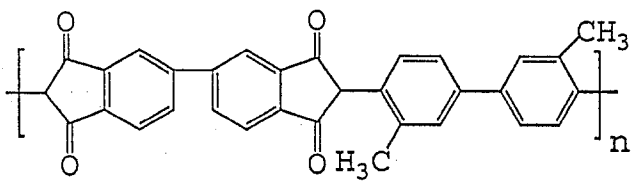

These three polyimides, BPDA-PFMB, BPDA-DMB and BPDA-OTOL, were synthesized using the same dianhydride (BPDA) with different diamines. Both PFMB and DMB possess pendent groups at 2 and 2′ positions. In the case of PFMB, the pendent groups are trifluoromethyl groups while for DMB they are methyl pendent groups. On the other hand, in the case of OTOL, the pendent groups are methyl groups at 3 and 3′ positions. It is particularly interesting to study the effect of chemical structure changes in these three polyimides on the crystal structure and properties of as-spun, annealed and drawn fibers. These structural parameters are closely associated with the thermal shrinkage behavior.

## Experimental

### *Preparation of polyimides and fibers*

Polyimides with 10% (*w/w*) concentration were synthesized from 3,3′,4,4′-biphenyltetracarboxylic dianhydride (BPDA) and one of the diamines at elevated temperature (200°C) in *m*-cresol or *p*-chlorophenol solution *via* a one-step polymerization method [5, 6]. During the polymerization, the poly(amic acid) precursors were not isolated, and the imidization process occurred almost simultaneously during the polymerization. When the polyimide solutions were cooled to room temperature, they underwent a liquid-liquid phase separation to form a gel-like structure [7, 8]. Fibers were spun from the isotropic solution via a dry jet-wet fiber spinning method in our laboratory. It includes a spinning head, spinneret, coagulation bath and winder. Draw ratio were controlled by a zone drawing in air between 380–420°C. As-spun fibers could be drawn up to ten times.

### *Instrument and experiments*

Wide angle X-ray diffraction (WAXD) fiber patterns were collected using either a Siemens two-dimensional detector or a flat vacuum camera with Ni filtered $CuK_\alpha$ X-ray radiation. The distance between the sample and detector was calibrated using 325 mesh size silicon powder with a diffraction 2θ angle of 28.46°. The degree of orientation is measured from the Hermans equation [11].

$$f_x = [3\ (\cos^2\Phi) - 1]/2$$

Cosine value of average orientation angle

$$(\cos^2\Phi) = \frac{\int_0^{90^\circ} I \cos^2\Phi \sin\Phi\, d\Phi}{\int_0^{90^\circ} \sin\Phi\, d\Phi}$$

The crystallinity was calculated with the formula as follows:

$$X_{cr} = \int_{5^\circ}^{35^\circ} I_{cr}\,(2\theta)\,\mathrm{d}(2\theta) \Big/ \int_{5^\circ}^{35^\circ} I_{cr}\,(2\theta)\,\mathrm{d}(2\theta) + \int_{5^\circ}^{35^\circ} I_{am}\,(2\theta)\,\mathrm{d}(2\theta)$$

$I_{cr}$, $I_{am}$ X-ray diffraction intensity contributed by crystalline and amorphous regions.

Density measurement were carried out by using a density gradient column of carbon-tetrachloride and *n*-hexane providing a density range between 1.2–1.5 g $cm^{-3}$.

The thermomechanical (TMA) properties of the fibers were measured using a Seiko stress-strain thermal mechanical analyser (TMA/SS100). The extension mode was used for the fibers to determine the thermal shrinkage behavior. Non-isothermal experiments at zero initial stress and zero initial strain were conducted on the TMA at a heating rate of 20°C $min^{-1}$.

## Results and discussion

### *Crystal unit cell determinations in the polyimide fibers*

Figures 1a–1c show WAXD fiber patterns for as-spun BPDA-PFMB, BPDA-DMB and BPDA-OTOL fibers. It is evident that BPDA-PFMB as-spun fibers do not exhibit preferential orientation along the meridian direction. Only a diffused ring pattern can be observed, indicating a more or less random orientation of the noncrystalline regions in the fibers (Fig. 1a). A very small percentage of crystallinity can be seen. However, in the case of BPDA-OTOL as-spun fibers, a moderate degree of crystallinity as well as crystalline and noncrystalline orientation is found. Sharp reflections can be observed in the WAXD fiber pattern (Fig. 1c). The as-spun BPDA-DMB fibers seem to be an intermediate case but more similar to BPDA-PFMB fibers (Fig. 1b). These results indicate that BPDA-OTOL is relatively easy to crystallize during the fiber spinning compared with the other two polyimides. The BPDA-DMB fibers followed by the BPDA-PFMB fibers are the most difficult to crystallize. Note that the difference in the chemical structures between BPDA-DMB and BPDA-OTOL polyimides lies only in the methyl group positions (2,2′- *vs.* 3,3′-substituents). This position difference affects the crystallization process during fiber spinning. One may speculate that the 3,3′-substituents possess less steric hindrance and therefore, the chain molecules are less rigid and relatively easy to incorporate into the crystal lattice. On the other hand, both BPDA-PFMB and BPDA-DMB have the pendent groups at the 2 and 2′ positions in the diamines, but differ in pendent group size and polarity. These differences also substantially influence the ability of the material to crystallize during fiber spinning.

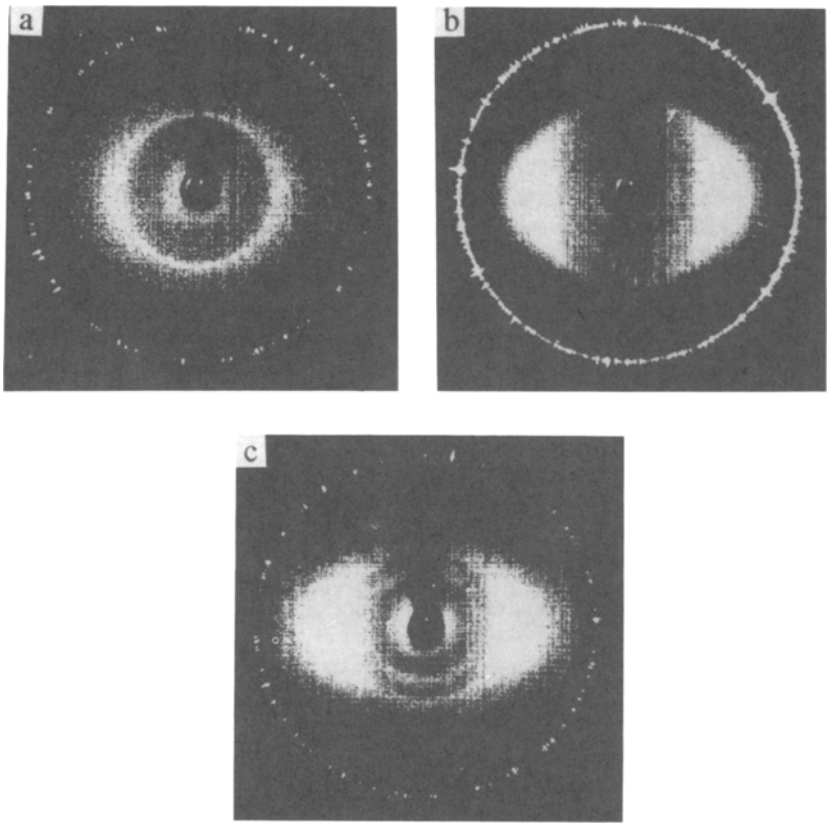


**Fig. 1** Set of WAXD patterns of as-spun (a) BPDA-PFMB fibers, (b) BPDA-DMB fibers, and (c) BPDA-OTOL fibers

From the processing point of view, crystallization may greatly affect the annealing and drawing processes and consequently, the ultimate mechanical properties. It is desirable to achieve a high degree of orientation during the initial stages of spinning prior to crystallization in order to obtain the maximum tensile properties. Therefore, a slower crystallization process may facilitate better molecular orientation. We predict that BPDA-OTOL should possess the lowest tensile properties among the three fibers tested due to the smallest amount of orientation in the fibers prior to crystallization. Experimental data shows that indeed, this prediction is correct [4, 9].

Figures 2a–2c are the WAXD fiber patterns for highly drawn and annealed BPDA-PFMB, BPDA-DMB and BPDA-OTOL fibers. They exhibit sharp Bragg reflections on the equator and several layer lines, indicating the existence of

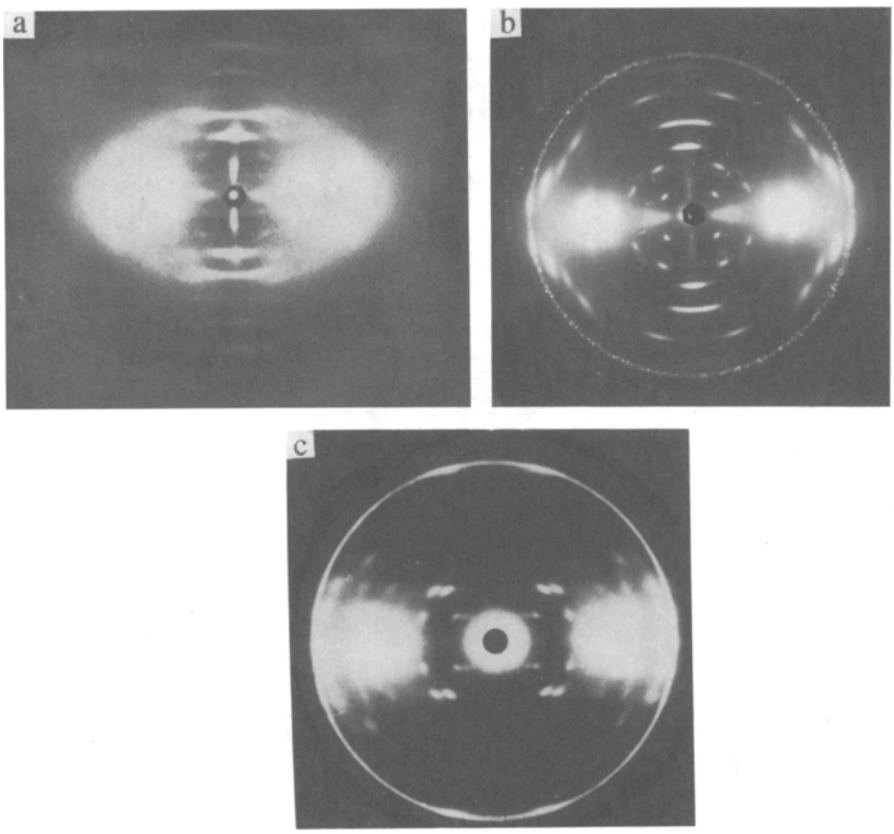


**Fig. 2** Set of WAXD patterns of highly drawn and annealed (a) BPDA-PFMB fibers, (b) BPDA-DMB fibers, and (c) BPDA-OTOL fibers

three-dimension order. Observed values of $d$-spacings and 2θ reflection angles for BPDA-OTOL fibers are listed in Table 1. The unit cell data for the other two polymers have been reported previously [1, 3]. In this table, calculated data are also included based on the crystal unit cell lattice dimensions. To determine the crystal unit cell, a conversion of diffraction spots in Cartesian coordinates ($X$ and $Y$) to reciprocal coordinates ($X^*$ and $Y^*$) in a reciprocal crystal lattice can be conducted through the relationships.

$$X^* = [2 - Y^{*2} - 2(1 - Y^{*2})^{1/2} \cos(2\theta)]^{1/2} \quad \text{and} \quad Y^* = Y/(Y^2 + R^2)^{1/2}$$

where $R$ is the distance between the sample and X-ray film, $Y$ is the height of the reflection spot from its equatorial line, and 2θ is the diffraction angle. For a triclinic lattice, the $Y^*$ values further indicate the distances between different

**Table 1** Experimental and calculated crystallographic parameters of the triclinic unit cell for highly drawn BPDA-OTOL fibers*

| | 2θ/° | | *d*-spacing /nm | | |
|---|---|---|---|---|---|
| (*hkl*) | Exp. | Calc. | Exp. | Calc. | Intensity |
| 110 | 8.66(9) | 8.70(3) | 1.02(0) | 1.01(6) | w |
| 220 | 17.3(5) | 17.4(6) | 0.51(1) | 0.50(8) | vs |
| 310 | 21.1(0) | 21.0(9) | 0.42(1) | 0.42(1) | s |
| $4\bar{1}0$ | 27.4(4) | 27.4(1) | 0.32(5) | 0.32(5) | s |
| 001 | 6.79(9) | 6.79(7) | 1.30(0) | 1.30(0) | m |
| $1\bar{1}1$ | 8.02(2) | 8.01(3) | 1.10(2) | 1.10(3) | m |
| $\bar{1}11$ | 13.0(6) | 13.0(6) | 0.67(8) | 0.67(8) | m |
| 141 | 20.8(0) | 20.7(2) | 0.42(7) | 0.42(9) | s |
| $22\bar{1}$ | 22.9(2) | 22.8(5) | 0.38(8) | 0.38(9) | m |
| 431 | 27.3(6) | 27.2(8) | 0.32(6) | 0.32(7) | m |
| $2\bar{1}2$ | 12.0(9) | 12.1(0) | 0.73(2) | 0.73(1) | s |
| 012 | 13.5(4) | 13.5(4) | 0.65(4) | 0.65(4) | s |
| 412 | 19.2(9) | 19.2(2) | 0.46(0) | 0.46(2) | w |
| $03\bar{2}$ | 23.1(4) | 23.1(9) | 0.38(4) | 0.38(4) | m |
| $\bar{2}22$ | 26.5(2) | 26.2(9) | 0.33(6) | 0.33(9) | m |
| $3\bar{3}3$ | 24.2(5) | 24.2(0) | 0.36(7) | 0.36(8) | m |
| 043 | 26.4(4) | 26.4(2) | 0.33(7) | 0.33(7) | w |
| 314 | 17.3(9) | 17.3(9) | 0.51(0) | 0.51(0) | m |
| 224 | 19.4(7) | 19.4(5) | 0.45(6) | 0.45(6) | m |
| 134 | 24.4(5) | 24.4(8) | 0.36(4) | 0.36(4) | m |
| 024 | 27.1(0) | 27.2(7) | 0.32(9) | 0.32(7) | m |

* The calculated 2θ and *d*-spacing are based on the triclinic unit cell of $a=2.02(1)$ nm, $b=1.73(0)$ nm, $c=2.03(9)$ nm, $\alpha=73.8°$, $\beta=40.7°$ and $\gamma=79.0°$

layers. One starts by finding an *hk0* reciprocal lattice net which is a parallelogram with edges of the $a^*$ and $b^*$ that account for the values determined from the equatorial reflections. In this case, $Y=0$, thus $Y_o^*=0$, and $X_o^*=[2-2\cos(2\theta)]^{1/2}$. The smallest distance between the center of the X-ray incident beam and the reflection spot corresponds to the lowest index. In trying to index the quadrant diffraction spots, one calculates the $Y^*$ values of the reflection spots on different layers. The distance values obtained from the different layers lead to a least common multiple which usually corresponds to the value of *c*-axis of the unit cell. Computer refinement is then conducted to achieve the fit with the least error between experimental results and calculated data based on a continuous refinement program starting with the unit cell shape and size obtained from the hand calculations. The crystal unit cell of BPDA-PFMB fiber is monoclinic with $a=1.28(2)$ nm, $b=0.91(8)$ nm, $c=2.02(5)$ nm and $\gamma=84°$.

The crystallographic density is 1.501 g $cm^{-3}$. This value fits well with the experimentally observed density data around 1.48 g $cm^{-3}$. The unit cells of both BPDA-DMB and BPDA-OTOL crystals are triclinic. For BPDA-DMB crystals, it is $a=2.04(8)$ nm, $b=1.52(9)$ nm, $c=4.00(2)$ nm, $\alpha=62.1°$, $\beta=52.2°$ and $\gamma=79.6°$ while for BPDA-OTOL fibers, the unit cell lattice possesses $a=2.02(1)$ nm, $b=1.73(0)$ nm, $c=2.03(9)$ nm, $\alpha=73.8°$, $\beta=40.7°$ and $\gamma=79.0°$. The crystallographic densities for these two fibers are 1.422 g $cm^{-3}$ and 1.401 g $cm^{-3}$, respectively. The experimental density data are around 1.39 g $cm^{-3}$ for BPDA-DMB fibers and 1.37 g $cm^{-3}$ for BPDA-OTOL fibers.

Among these three WAXD fiber patterns, the BPDA-PFMB shows the smallest number of the reflections. This may be associated with a difficulty of chain packing in the BPDA-PFMB crystals due to a greater steric hindrance introduced by the trifluoromethyl pendent groups in the PFMB diamine in comparison with the methyl pendent groups in the DMB and OTOL diamines. This speculation can also be supported by the fact that the crystallinity of highly drawn and annealed BPDA-PFMB fibers is about 60% which is about 10% lower than that of BPDA-DMB fibers [1, 3]. On the other hand, the BPDA-DMB and BPDA-OTOL WAXD fiber patterns exhibit a number of sharp reflections. The molecular structural difference between BPDA-DMB and BPDA-OTOL is the position of the two methyl pendent groups (the 2 and 2′ *vs.* the 3 and 3′ positions). The WAXD crystallinities of these two fibers are in the similar, at approximately 70% within the experimental error. This indicates that ultimate crystallinity is critically associated with the size and polarity of the side pendent groups. In addition, crystallization kinetics are also determined by the position of these groups. On *c*-axes, BPDA-OTOL has only one chemical repeat unit comparing with BPDA-DMB having 2 repeat units, it obviously caused by more flexible chain for BPDA-OTOL.

### *Thermal shrinkage behaviors*

Figures 3a–3c show the thermal shrinkage strain developed in the three as-spun polyimide fibers under zero tension at a heating rate of 20°C $min^{-1}$. From the figures, two shrinkage processes (a negative change of the sample length) and one elongation process (a positive change of the sample length) are observed. These two shrinkage processes occur in the low and high temperature ranges while the elongation process occurs between them at around 450°C. The shrinkage process at low temperature is generally weak in magnitude, which may reflect microbrownian motion of the segments in the noncrystalline region of chain molecules. This segmental motion may be associated with a secondary relaxation appearing at 100–200°C in the polyimide fibers [2, 3] and/or a relaxation of a small amount of internal stresses frozen into the as-spun fiber during spinning.

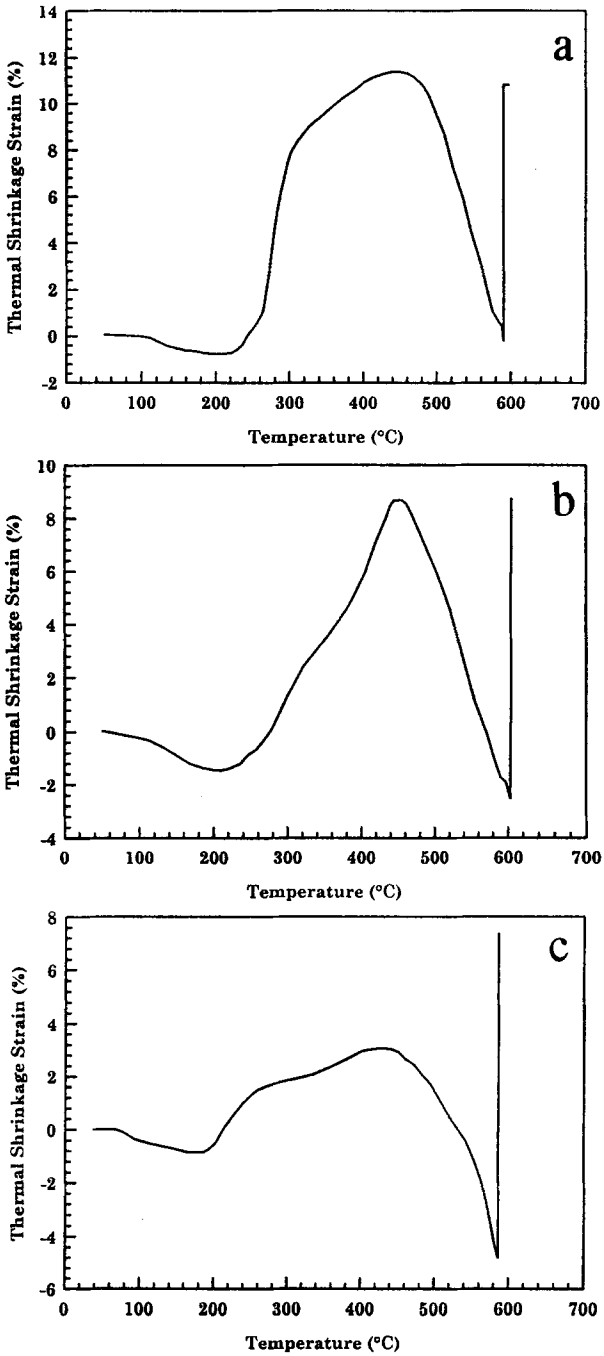


**Fig. 3** Set of thermal shrinkage strain curves for as-spun (a) BPDA-PFMB fibers, (b) BPDA-DMB fibers, and (c) BPDA-OTOL fibers

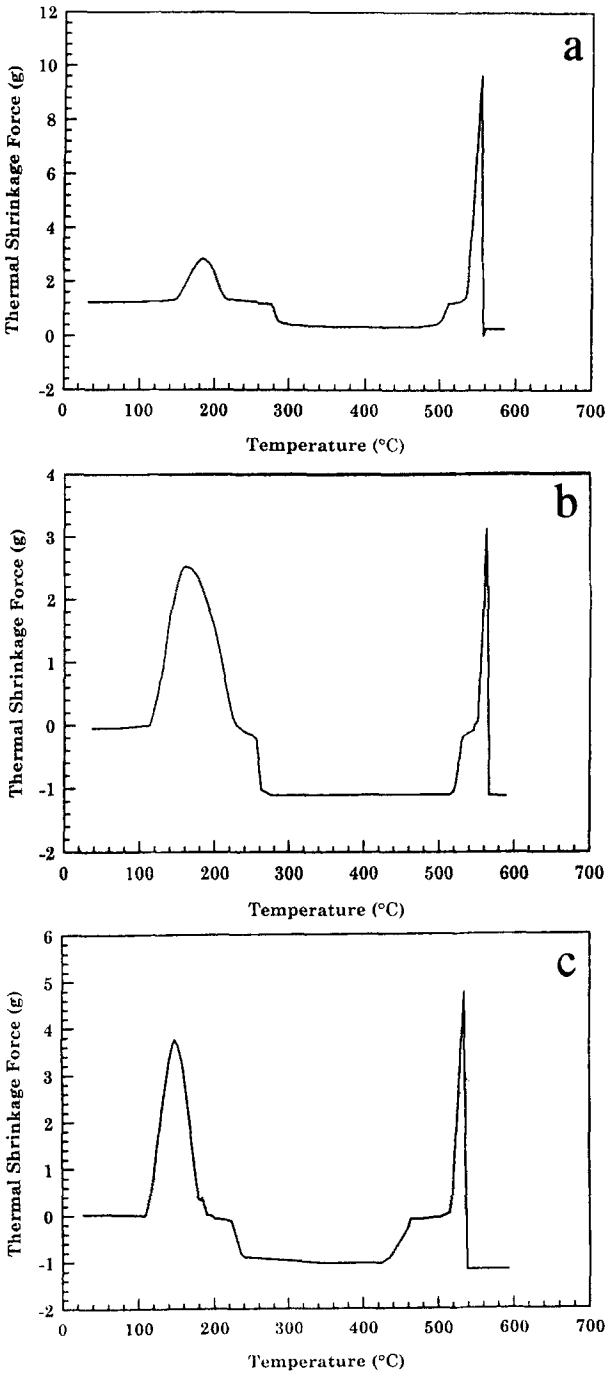


**Fig. 4** Set of thermal shrinkage stress curves for as-spun (a) BPDA-PFMB fibers, (b) BPDA-DMB fibers, and (c) BPDA-OTOL fibers

As the temperature increases, the fibers show an elongation without applied tension. This phenomenon has been observed by Zhubanov *et al. via* their dilatometric method in polyimide fibers and has been termed "self-elongation" [10]. It seems to be a unique characteristic of polyimide fibers. The degree of self-elongation is dependent upon pre-existing structures in the fibers. Among the as-spun fibers during heating the "self-elongation" of BPDA-PFMB fibers is most prominent while that of the BPDA-OTOL fiber is the least. This seems to imply that a relatively loose chain packing with less orientation and ordered structure yields a higher degree of self-elongation.

Figures 4a–4c represent the thermal shrinkage stress appearing in the three polyimide fibers under a fixed sample length at the same heating rate. They show two shrinkage stress processes, which correspond to the shrinkage processes in the thermal shrinkage strain behavior observed in Fig. 3a–3c.

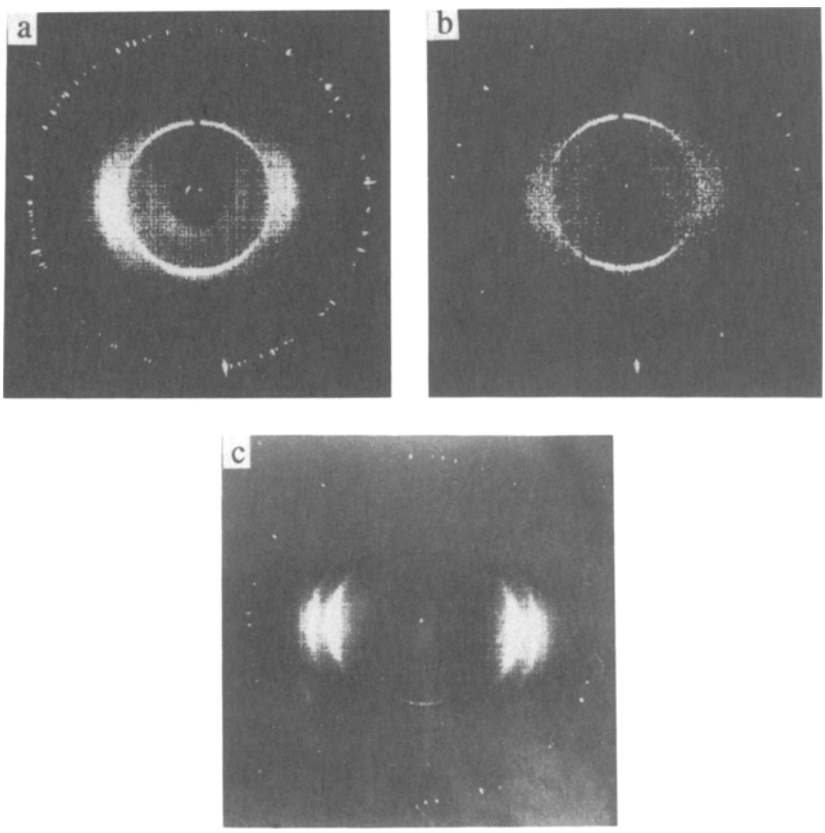


**Fig. 5** Set of WAXD patterns of annealed as-spun (a) BPDA-PFMB fibers, (b) BPDA-DMB fibers, and (c) BPDA-OTOL fibers

However, no shrinkage stress can be found at the temperature where the self elongation is observed. The magnitude of the second thermal shrinkage process is much more pronounced than that of the first one. This process may be associated with a premelting of the crystals under stress which should be related to the motion of the polymer chains in the ordered region.

During the self-elongation, the fibers exhibit structural changes. Figures 5a–5c are WAXD fiber patterns taken from the annealed as-spun fibers which possess the same thermal history as the samples in TMA measurements. Degrees of orientations in the noncrystalline region are enhanced. As-spun BPDA-PFMB fibers possess the lowest degree of orientation at 0.55. A change of 0.12 is achieved after annealing. However, in as-spun BPDA-OTOL, the annealing process does not significantly affect the degree of orientation. A change of 0.02 is found. This indicates that the pre-existing structure in the fiber largely influences this change. Furthermore, for BPDA-DMB and BPDA-OTOL fibers, the annealing process leads to a further development of the crystallinity. This again, reveals that these two polyimides are capable of crystallizing with relative ease compared to BPDA-PFMB.

## Conclusion

Three aromatic polyimide fibers have been spun and their crystal unit cell dimensions and lattices have been determined. In BPDA-PFMB and BPDA-DMB fibers, the difference of the crystal structures is caused *via* the substituting fluorines with hydrogens in the methyl pendent groups. On the other hand, BPDA-DMB and BPDA-OTOL fibers show different crystal structures due to the different substituent positions of the methyl groups. The three polyimide fibers exhibit self-elongation behavior during annealing at high temperatures, which is associated with the changes in structure and orientation in the fibers. It is important to recognize that the pre-existing structure in as-spun fibers critically affects the final fiber mechanical properties due to a competition between the crystallization and orientation processes during fiber formation.

* * *

This work was supported by SZDC's Presidential Young Investigator Award from the National Science Foundation (DMR-9175538) and NSA/EPIC/Ohio Industry Center of Molecular and Microstructure Composites at Case Westen Reserve University and The University of Akron.

## References

1 S. Z. D.Cheng, Z. Q. Wu, M. Eashoo, S. L.-C. Hsu and F. W. Harris, Polymer, 32 (1991) 1803.
2 M. Eashoo, D. X. Shen, Z. Q. Wu, C. J. Lee and F. W. Harris, Polymer, 33 (1993) 3209.

3 M. Eashoo, Z. Q. Wu, A. Q. Zhang, D. X. Shen, C. Tse, F. W. Harris, S. Z. D. Cheng, B. S. Hsiao and K. H. Gardner, Macromol. Chem. Phys., 195 (1994) 2207.
4 D. X. Shen, Z. Q. Wu, J. Liu, L. X. Wang, S. K. Lee, F. W. Harris and S. Z. D. Cheng, Polymers & Polymer Composites, 2 (1994) 149.
5 F. W. Harris in "Polyimides'; D. Wilson, H. D. Stenzenberger, P. M. Hergenrother Eds., Chapman and Hall, New York 1989, Chapt. 1, pp. 1-37.
6 S. Z. D. Cheng and F. W. Harris, "Polyimide fibers, Aromatic" International Encyclopaedia of Polymer Composite, 1991, Vol.6, pp. 293-309.
7 S. K. Lee, Ph.D. Dissertation, Department of Polymer Science, The University of Akron, Akron, Ohio, 44325-3909, 1995.
8 S. K. Lee, S. Z. D. Cheng, Z.-Q. Wu, C. J. Lee, F. W. Harris, T. Kyu and J.-C. Yang, Polym. Interl., 30 (1993) 115.
9 S. Lee, Ph.D. Dissertation, Department of Polymer Science, The University of Akron, Akron, Ohio, 44325-3909, 1993.
10 B. A. Zhubanov, B. K. Donenov, L. N. Korzhavin, G. I. Boiko and M. B. Umerzakov, Khim. Volokno (Russ.), 4 (1990) 44.
11 M. Kakudo and N. Kasai, X-ray Diffraction by Polymers, Elsevier Publishing Co. New York 1972, p. 255.